Seasonal Phase Relationships between Sea Surface Salinity, Surface Freshwater Forcing and Ocean Surface Processes

F. M. Bingham[1], S. K. Brodnitz[2]

[1]University of North Carolina Wilmington, Center for Marine Science and Department of Physics & Physical Oceanography

[2]InfluxData

Corresponding author: Frederick M. Bingham (binghamf@uncw.edu)

Key Points:

- We examine the seasonal phase relationship between sea surface salinity, surface freshwater forcing, advection and vertical entrainment
- Sea surface salinity should be 3 months behind the surface freshwater forcing, but we find it is generally closer to 1-2 months
- The addition of advection and vertical entrainment can rectify the phase and bring the surface salinity in line with forcing processes

Abstract

Sea Surface Salinity (SSS) can change as a result of surface freshwater forcing (FWF), or internal ocean processes such as upwelling or advection. At the seasonal scale, SSS should follow FWF by ¼ cycle, or 3 months, if FWF is the primary process controlling it at the seasonal scale. In this paper we compare the phase relationship between SSS and FWF (i.e. evaporation minus precipitation over mixed layer depth) over the global (non-Arctic) ocean using in situ SSS and satellite evaporation and precipitation. We find that instead of the expected 3 month delay between SSS and FWF, the delay is mostly closer to 1-2 months, with SSS peaking too soon relative to FWF. We then compute monthly vertical entrainment and horizontal advection terms of the upper ocean salinity balance equation and add their contributions to the phase of the FWF. The addition of these processes to the seasonal upper ocean salinity balance brings the phase difference between SSS and the forcing processes closer to the expected value. We do a similar computation with the amplitude of the seasonal SSS and the forcing terms, with less definitive results. The results of this study highlight the important role that ocean processes play in the global freshwater cycle at the seasonal scale.

Plain Language Summary

Sea surface salinity (SSS) is an indicator of the global cycle of freshwater at the seasonal scale. It can change in response to surface input of freshwater from rainfall or evaporation, or from processes internal to the ocean. If SSS were completely controlled by rainfall and evaporation it would have a seasonal cycle that lags the combination of rainfall and evaporation by 3 months. However, by studying SSS, evaporation and precipitation, we find that over much of the ocean the actual lag is closer to 1-2 months. This means that SSS peaks too soon relative to the surface input/output of freshwater. To understand this further, we compute some terms related to processes internal to the ocean at the seasonal scale, including the motion of water both horizontally and vertically. The addition of these terms brings the seasonal cycle of SSS closer to balance with the processes which can change it. We find that vertical motion is especially important in this regard. Our study highlights the importance of ocean processes in the global seasonal balance of freshwater.

1 Introduction

The lower atmosphere and upper ocean are connected through fluxes of freshwater that freshen or salten the ocean, or add or subtract moisture from the atmosphere through evaporation and precipitation. These fluxes occur on many different time and space scales, and can help drive the circulation of both the atmosphere and ocean through the transfer of buoyancy and latent heat (Huang & Schmitt, 1993). One of the most important time scales for ocean surface freshwater fluxes is the seasonal (Bingham & Lee, 2017), which is related to such important phenomena as monsoon circulation and atmospheric rivers (Hoffman et al., 2022). The atmosphere lifts water off the surface of the ocean on a seasonal basis and carries it either onto land or to a different part of the ocean. The globally-averaged amplitude of this extraction of water is something like 10 mm of equivlalent sea surface height as measured by ocean mass (Chambers et al., 2004), altimetry (Minster et al., 1999) or ocean salinity (Bingham et al., 2012). It is likely, however, that the amplitude of the seasonal extraction is much larger in some regions than others, as the atmosphere transports water on a seasonal basis from one part of the ocean, say one hemisphere or ocean basin, to another.

Because the atmosphere and ocean are so closely connected through freshwater fluxes, we expect those fluxes to be reflected in the properties of the surface ocean, namely the salinity. As the ocean surface freshwater flux (evaporation minus precipitation) increases or decreases throughout the annual cycle, the surface salinity should increase or decrease as well with about a ¼ cycle, or three month, phase delay (Delcroix et al., 1996). This assumes that other ocean processes are not important on a seasonal time scale. Yu (2011) however, found that other processes are important for determining surface salinity, particularly Ekman and geostrophic transport, and vertical mixing/entrainment. So to the extent that the timing and amplitude of surface salinity changes do not match that of surface freshwater flux, the surface salinity may be determined by seasonal-scale processes internal to the ocean.

The seasonal cycle of the surface salinity of the ocean (SSS) has been the subject of a number of studies. On a global scale, patterns of amplitude and phase of the seasonal cycle of SSS have been presented (Bingham et al., 2012; Yu et al., 2021; Boyer & Levitus, 2002, Song et al., 2015; Chen et al., 2018) showing regions where the seasonal cycle is strong, i.e. the tropics, northern and southern Indian Ocean, Amazon and Congo River plumes, the Arctic, etc. SSS tends to be highest in the late winter / early spring months of March and September (Bingham et al., 2012). Maps of amplitude and phase have also been presented on a regional level for many locations, including: the global tropics (Bingham et al., 2021), global subtropics (Gordon et al., 2015), Pacific basin (Bingham et al., 2010), subtropical North Atlantic (Bingham et al., 2014), Atlantic basin (Levitus, 1986; Sena Martins et al., 2015), tropical Atlantic (Dessier & Donguy, 1994), Indian basin (Köhler et al., 2017), North Indian (Rao & Sivakumar, 2003), and tropical Indian (Donguy & Meyers, 1996; Maes & O'Kane, 2014). The result of these disparate studies is that we have a good idea of where the seasonal cycle of SSS is large, and how much variance it represents, over much of the globe. However, for the most part these studies do not relate the amplitude and phase of the seasonal cycle to that of the forcing, specifically evaporation minus precipitation (E-P).

Many other studies present the climatological seasonal balance of SSS as budgets (e.g. Delcroix et al., 1996; Yu, 2011), indicating the importance of the salinity tendency, gain and loss of freshwater at the surface, vertical and horizontal mixing, horizontal advection, etc. These are usually done regionally, in such areas as: the global subtropics (Johnson et al., 2016), tropical Atlantic (Camara et al., 2015; Da-Allada et al., 2013; Da-Allada et al., 2014; Foltz & McPhaden, 2008; Foltz et al., 2004), subtropical North Atlantic (Dong et al., 2015; Dohan et al., 2015; Farrar et al., 2015; Foltz & McPhaden, 2008), tropical Indian (Da-Allada et al., 2015; Köhler et al., 2017), south Indian subtropics (Wang et al., 2020), Southern Ocean (Dong et al., 2009), tropical Pacific (Hasson et al., 2013b; Farrar and Plueddemann, 2019), and South Pacific subtropics (Hasson et al., 2013a). There are also a couple of studies of the salinity balance of the ocean globally (Vinogradova & Ponte, 2013; Yu, 2011). In some of these studies, the seasonal cycle is more or less closed (e.g. Da-Allada et al., 2015; Dong et al., 2015) and in others it is not (e.g. Wang et al., 2020). When the SSS budget is climatologically closed, we would expect that the salinity tendency would peak at exactly the same time as the sum of all of the other terms, or we would expect the SSS itself to peak 3 months, or ¼ cycle after the sum of the other terms (Delcroix et al., 1996; Reverdin et al., 2007; Bingham et al., 2010). However, this may not be the case everywhere, as Bingham et al. (2012) found that SSS systematically peaks about 1-2 months ahead of this expected three month phase delay.

What we are interested in here is the amplitude and phase relationship between SSS and surface forcing on a seasonal basis, with additional modulation by internal ocean processes such as advection and vertical entrainment. Many of the studies just cited do get to this question on a local level, but not on a global basis in a way we could use to quantify the large-scale movement of water off of the ocean surface and onto land or to a different part of the ocean. As a typical example, Foltz and McPhaden (2008) examine the SSS balance in three areas in the tropical and subtropical North Atlantic. They compare the salinity tendency with the sum of vertical advection, horizontal advection and surface moisture flux in these areas. The results are mixed. In one area, in the central subtropical ocean, there is little seasonal variability of any of these quantities. In the other two areas, the western and tropical ocean, there are robust seasonal cycles, with the amplitude of the tendency being similar to those of the sum of the other terms. Most importantly for this work, there is a phase offset. The tendency peaks about 2 months earlier than the sum of the other terms. Phase offsets like this are common in these kinds of SSS seasonal budget evaluation studies (e.g. Dong et al., 2008, Hasson et al., 2013b).

As mentioned above, the phase and amplitude of the annual cycle of SSS or its tendency has been displayed in many studies, but there has been little attempt to systematically relate these to that of the forcing or other terms in the upper ocean salinity balance. Bingham et al. (2012) did try this, and found, as mentioned above, a systematic offset of about 1-2 months between peak SSS and peak surface forcing, versus the expected 3 months. They also found that the amplitude of the SSS seasonal cycle was larger than that of the surface forcing. This study was done with a crude, pre-satellite SSS field and mostly pre-Argo dataset. The SSS seasonal cycle has become much better understood over the past decade with the advent of satellite measurement of SSS (Yu et al., 2021; Vinogradova et al., 2019). This and improved precipitation (Skofronick-Jackson et al., 2018) and evaporation (Yu et al., 2007) datasets make it timely to examine the seasonal phase and amplitude relationships between SSS, surface freshwater forcing (FWF) and internal ocean processes. Of these two, we find the phase relationship more interesting and understandable from the datasets we have.

2 Data and Methods

The purpose of this study is to determine the phase relationship between SSS and other terms of the salinity balance equation, i.e. surface freshwater forcing, advection and vertical entrainment. Thus we need to detail the data sources, method for computing the terms, and the method for computing the seasonal harmonics. The upper ocean salinity balance equation can be expressed in many forms. We follow the simple formulation of Bingham et al. (2010) and Delcroix et al. (1996), i.e.

$$\frac{\partial S}{\partial t} = \frac{S_0(E-P)}{h} - \vec{u} \cdot \nabla S - w\frac{\partial S}{\partial z} \quad (1)$$

where S is the upper ocean salinity, t is time, S_0 is a reference value of S set to 35, E is evaporation, P is precipitation, h is the mixed-layer depth, $\vec{u}$ the horizontal velocity, w the vertical velocity and z the vertical coordinate. The first term on the right-hand-side of (1) is the FWF, the second term is advection and the third is the vertical entrainment. We will estimate these terms on a global basis using in situ and satellite data and determine their seasonal harmonics.

148 ### 2.1 Data sources

149 The datasets we used were:

150 • A gridded in situ salinity product derived from Argo floats (the "RG" data; Roemmich &
151 Gilson, 2009). This is a monthly product on a 1°X1° grid.

152 • OAFlux evaporation (Yu & Weller, 2007).

153 • MIMOC mixed layer depth (Monthly Isopycnal and Mixed-layer Ocean Climatology;
154 Schmidtko et al., 2013). This is a climatology, not a time series. We tried some other time
155 series mixed layer products but found them not useful for our purposes.

156 • GPM IMERG precipitation (Skofronick-Jackson et al., 2018).

157 • OSCAR (Ocean Surface Current Analyses Real-time) surface velocity (Bonjean &
158 Lagerloef, 2002).

159 • Ekman upwelling produced by the NOAA Coastwatch program. These are monthly 0.25°
160 values of vertical velocity at the surface derived from wind stress data.

161

162 We averaged all data to a monthly 1° grid, with latitude ranging from 63°S to 64°N. The salinity
163 and evaporation data were initially available every degree centered on half degree increments,
164 and we regridded it to be centered on whole degree increments. The mixed layer depth data was
165 available every half degree and we subsampled the points centered on whole degrees to get a
166 consistent grid.

167 ### 2.2 Computing seasonal harmonics

168 For the SSS, the FWF, and the FWF combined with advection and entrainment, we
169 calculated the harmonics in the same way, following Bingham et al. (2010) and Yu et al. (2021).
170 We looped through all latitude and longitude values on the worldwide 1° grid and pulled out the
171 time series at each location. We computed a regression on the annual and semiannual harmonics
172 combined for each time series. The regression returned 5 coefficients, which we used to calculate
173 the amplitude and phase of the annual and semiannual harmonics. We also calculated the r^2 value
174 for both the annual and semiannual harmonic at each point, using the variance of the time series
175 and of the annual and semiannual fits. We then calculated the f-statistic from the r^2 values, and
176 the cumulative f-distribution from that. We considered fits with cumulative f-distribution values
177 greater than 0.9 and with more than a year of total data points at a location significant. The vast
178 majority of semiannual harmonic fits were not significant and we focus on annual harmonic
179 results in this paper. The results of this computation are the annual phase and amplitude of the fit
180 at each location, as well as whether the fit is significant. An example is shown in Figure 1, with
181 original SSS, entrainment/advection and FWF data and the harmonic fits.

182 Suppose that the salinity is a seasonally-varying sine function and the tendency is
183 completely balanced by a seasonally-varying FWF. S is then expressed as

184

185 $$S = A\sin(\omega t + \varphi) \quad (2)$$

where ω is $2\pi\ radians/year$, φ is the phase, t the time, and A the amplitude. The FWF is

$$FWF = Bsin(\omega t + \emptyset) \qquad (3)$$

where B is the amplitude of the FWF and $\emptyset$ is a different phase. Taking the derivative of S with respect to time, and setting $\frac{\partial S}{\partial t}$ and FWF equal to each other, we get

$$A\omega\cos(\omega t + \varphi) = Bsin(\omega t + \emptyset) \quad (4)$$

In order for this to balance we have to have $\emptyset = \varphi + \frac{\pi}{2}$. That is, the FWF leads S by ¼ cycle. We also have

$$A = \frac{B}{\omega} \quad (5)$$

So if we plot A, the amplitude of S vs. B, the amplitude of FWF, the slope should be $1/\omega$, i.e. $1/2\pi$.

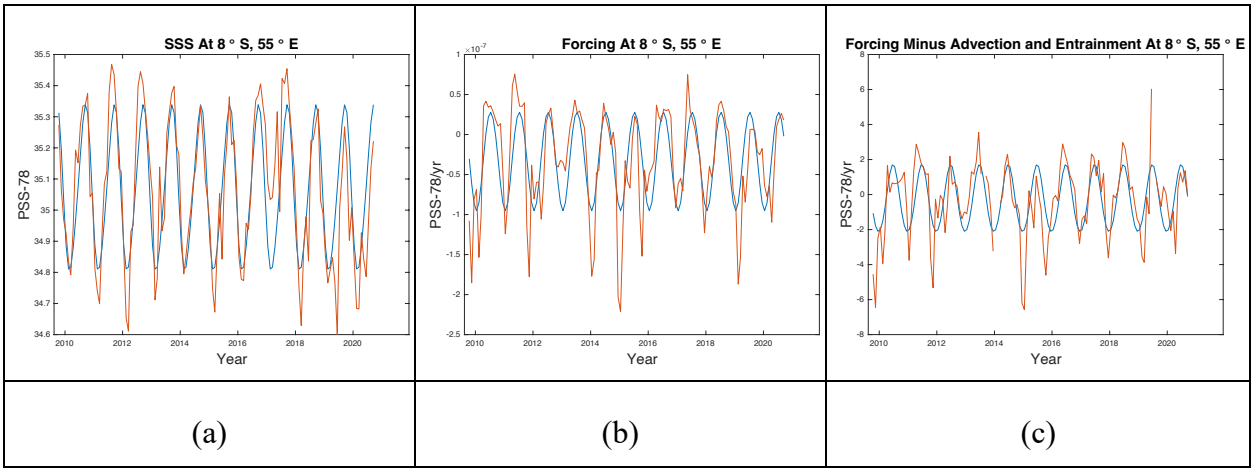

Figure 1: (a) Data (orange) and harmonic fit (blue) of SSS at grid point centered at 8°S 55°E. (b) Same as (a) but for FWF. (c) Same as (a) but for FWF combined with advection and entrainment.

2.3 Computing advection and entrainment

We calculated horizontal advection using the ocean velocity data set and the surface salinity. Horizontal advection is defined as the dot product of the surface velocity vector and the surface salinity gradient (equation 1). The OSCAR product consists of zonal and meridional components. Its time resolution is every 5 days, so we calculated monthly averages by directly averaging all the components separately at a given location in a given month. The grid for ocean velocity was at a 1° resolution and centered on every half degree. To calculate the dot product we needed the meridional and zonal partial derivatives of the surface salinity. The zonal partial derivative was calculated as the difference between the salinity at each grid point minus the salinity at the grid point with the previous longitude value, divided by the difference between them. This changed the centering in just the longitudinal direction to every half degree, so we

regridded in the latitudinal direction so every point was centered on the half degree in both directions, to be consistent with the velocity data. We calculated the meridional derivative in the same manner, finding the difference between points with different latitudes along longitude lines, dividing by distance, and regridding to every half degree. We then calculated advection at every half degree by multiplying the zonal and meridional components of the salinity gradient and the surface velocity, and finally regridded the advection to be centered on every whole degree.

The mean advection (Figure 2b) indicates the transformation of surface water as it flows from one part of the ocean to another. It is generally small compared to the surface forcing (Figure 2a) and vertical entrainment (Figure 2c), though it can be larger locally. It is large within intense western boundary currents such as the Gulf Stream, Kuroshio and Brazil-Malvinas Confluence, and also in the Antarctic Circumpolar Current at 35-45°S. It results in both freshening and saltening of the surface layer. There are bands of alternating impacts in the tropics.

We define vertical entrainment as the seasonal vertical velocity multiplied by the average vertical salinity gradient added to the seasonal vertical salinity gradient multiplied by the average vertical velocity.

$$S\frac{\partial w}{\partial z} = w'\frac{\overline{\partial S}}{\partial z} + \overline{w}\frac{\partial S'}{\partial z}$$

To calculate the vertical velocity we combined the upwelling and the vertical motion of the mixed layer base.

$$w' = w_E + \frac{\partial h}{\partial t}$$

where w_e is the Ekman upwelling velocity.

We subsampled the upwelling velocity grid to get upwelling values at whole degrees in the latitude range we were interested in. There was one month of data, August 2013, that has obviously incorrect values so we set that those values to null. To calculate the vertical motion of the mixed layer base at each location we subtracted the previous month's value from the current month's value and divided by the length of time in between the two time indices in seconds. This changed the centering in time so we then averaged every two monthly values again to get back to centering in the middle of months. We then combined the upwelling and vertical motion of the mixed layer base to get the vertical velocity. Because only water moving up into the mixed layer from below changes the salinity of the water in the mixed layer (Kraus & Turner, 1967; Yu, 2011), we only included positive vertical velocity in our calculations. We set all negative (downward) vertical velocity values to zero.We took the mean at each location across all the years analyzed for the average vertical velocity. We define entrainment as a change in salinity, not a movement of water.

For the vertical salinity gradient we compared the salinity at the surface and 30 m below the average mixed layer depth at each location from the RG data (Bingham et al., 2010). For the average gradient at each grid point we took the mean of the salinity at the surface minus the mean below the mixed layer depth, divided by the distance of 30m below the mixed layer depth. For the seasonal vertical salinity gradient we also subtracted the salinity 30m below the mixed layer depth from the surface salinity and divided by depth, with the salinity still varying in time.

252

253 $$\frac{\partial S'}{\partial z} = \frac{S(0) - S(MLD + 30)}{MLD + 30}$$

254 The average entrainment (Fig. 2c) shows that this process largely acts to increase the
255 salinity of the mixed layer. It is especially large in the tropics, on the eastern and western
256 boundary of the tropical Pacific and in the Indian Ocean. There are some areas, specifically in
257 the mid-latitude ocean subtropics where entrainment acts to freshen the mixed layer, where it is
258 underlain by fresher water. The magnitude of this is small compared to the intense upwelling of
259 salty water that occurs in the tropics (McCreary & Lu, 1994).

260

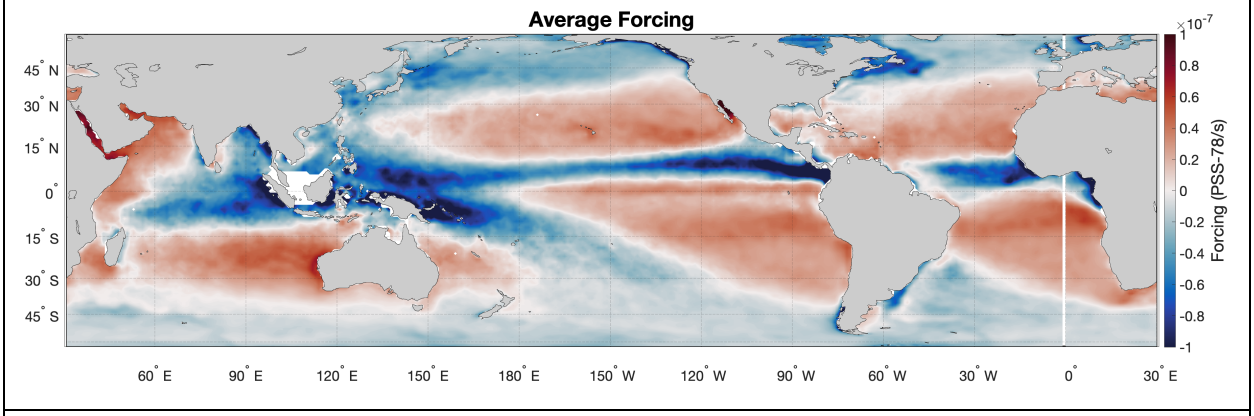
Average Forcing
45° N
30° N
15° N
0°
15° S
30° S
45° S
60° E
90° E
120° E
150° E
180° E
150° W
120° W
90° W
60° W
30° W
0°
30° E
×10^-7
1
0.8
0.6
0.4
0.2
0
-0.2
-0.4
-0.6
-0.8
-1
Forcing (PSS-78/s)

(a)

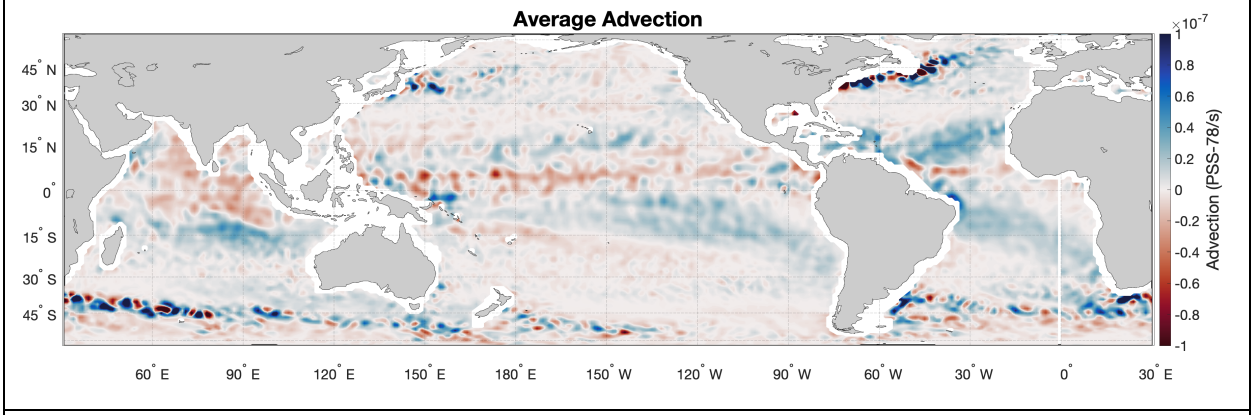
Average Advection
45° N
30° N
15° N
0°
15° S
30° S
45° S
60° E
90° E
120° E
150° E
180° E
150° W
120° W
90° W
60° W
30° W
0°
30° E
×10^-7
1
0.8
0.6
0.4
0.2
0
-0.2
-0.4
-0.6
-0.8
-1
Advection (PSS-78/s)

(b)

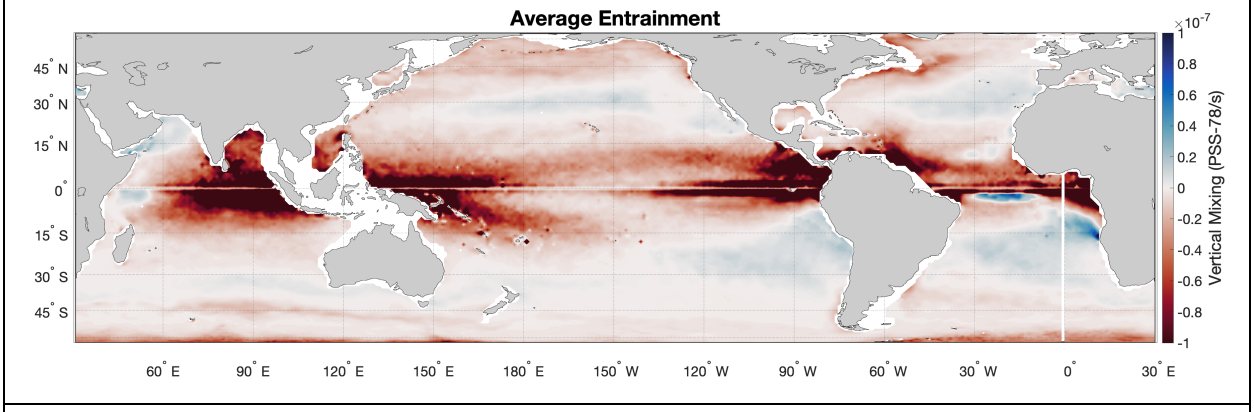
Average Entrainment
45° N
30° N
15° N
0°
15° S
30° S
45° S
60° E
90° E
120° E
150° E
180° E
150° W
120° W
90° W
60° W
30° W
0°
30° E
×10^-7
1
0.8
0.6
0.4
0.2
0
-0.2
-0.4
-0.6
-0.8
-1
Vertical Mixing (PSS-78/s)

(c)

Figure 2: (a) Map of average FWF over the full time span analyzed, October 2009 to September 2020. Color indicates PSS-78/s with scale at right. For reference, 1.0 X 10^{-7} PSS-78/s is equal to 3.2 PSS-78/year. (b) Same as (a) but for average advection and an inverted color scale so that red still indicates increasing salinity and blue indicates decreasing salinity. (c) Same as (b) but for average entrainment.

2.4 Computing forcing

As stated above, the mixed layer depth values are from a monthly average climatology. The picture of mean FWF (Figure 2a) can be compared to that of Schanze et al. (2010), who showed a very similar map of E-P. Large areas of excess precipitation are seen in the intertropical convergence zone in the Pacific and Atlantic, the South Pacific Convergence zone in the western South Pacific, the tropical Indian Ocean and at high latitudes. Excess evaporation occurs over large areas of the mid-latitude subtropics.

2.5 Computation of histograms

We computed the area of every one degree box within the latitude and longitude ranges we are using in order to normalize the histograms by area. Each histogram shows normalized areas of the ocean where the phase peaks in various months. We only plot areas with statistically significant fits, and both the significance and the area are considered separated for the salinity, the forcing, and the forcing combined with advection and entrainment.

3 Results

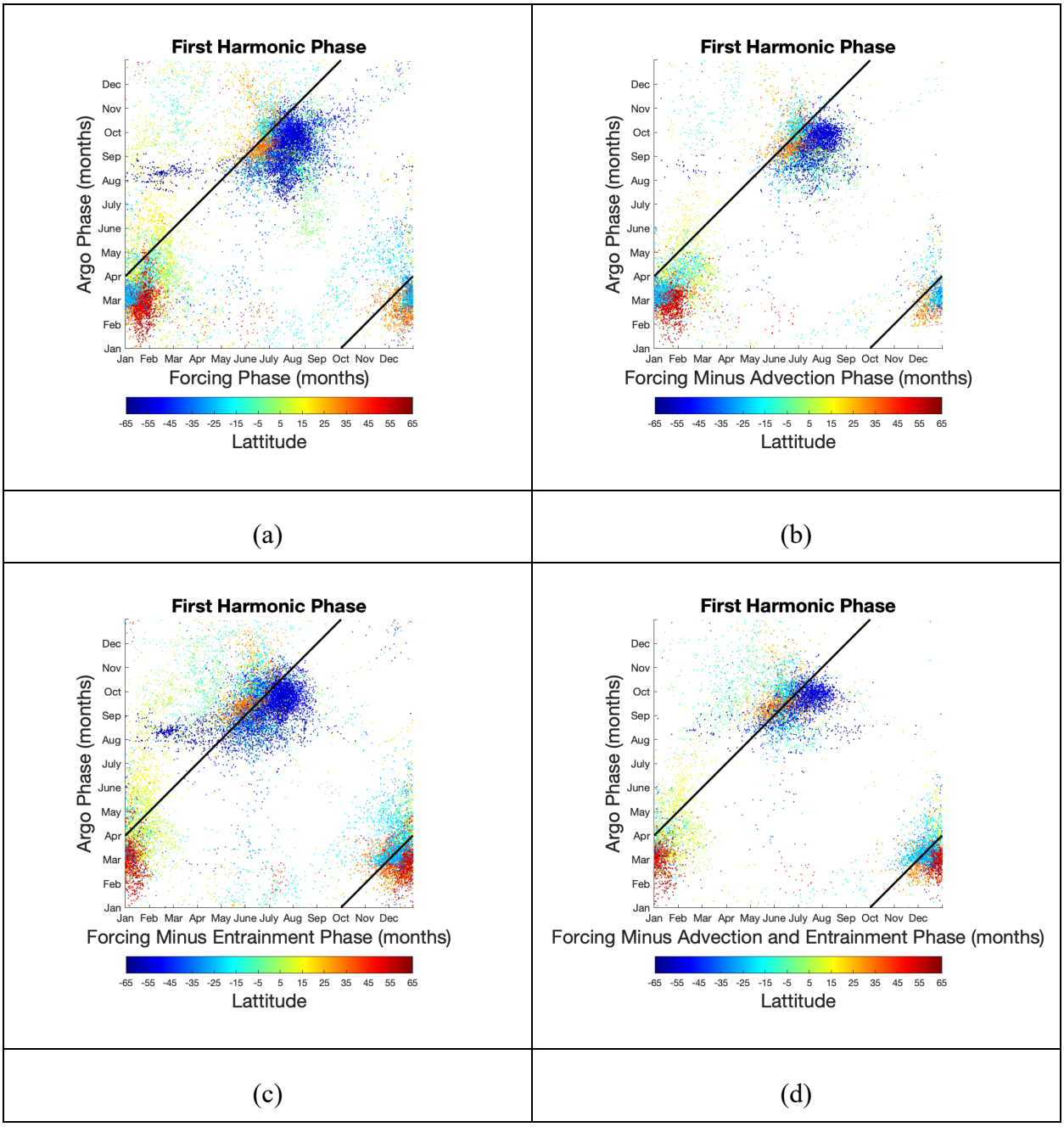

Figure 3: (a) Scatterplot comparison of harmonic phase (month of peak) for RG data vs. FWF. Each symbol is for one (1°) grid point, with symbols plotted only where there is a significant fit for both RG data and FWF. Colors of symbols indicate latitude of each point with scale at bottom. A black line indicates a 3 month lag between SSS and the FWF term. It shows the correspondence expected if the FWF totally determined the SSS. (b) Same as (a) but for

RG data vs. FWF combined with advection. (c) Same as (a) but for RG data vs. FWF combined with entrainment. (d) Same as (a) but for RG data vs. FWF combined with advection and entrainment.

The four scatterplots in Figure 3 show the annual phase of the surface salinity compared to the annual phase of various combinations of forcing terms. Figure 3a(b,c,d) has 18402 (10119, 17387, 9351) points. Adding in both advection and entraintment causes fewer locations within the ocean to have statistically significant annual harmonic fits.

Comparing just SSS and the FWF (Figure 3a) the majority of the global ocean does not have the FWF peaking with the expected 3 month phase lead over SSS. That is, one would expect the cloud of dots in Figure 3a to be centered around the black lines, which indicate 3 months of phase lag. Instead, the SSS systematically peaks too early in most areas by 1-2 months. This agrees with the result of Bingham et al. (2012). Another interesting aspect to the distribution shown is that for most of the ocean SSS peaks in the spring in either hemisphere. This can also be seen in the maps of Bingham et al. (2012) and Yu et al. (2021).

Adding in other terms of the salinity balance equation can change the picture. Considering FWF minus advection (Figure 3b), the cloud of points in the figure does not move much. Vertical entrainment has more impact. Including entrainment both by itself and along with advection does move the clusters of points closer to being centered around the 3-month expected lag. This suggests that entrainment does more than advection to delay the phase of the ocean's response to FWF. Grid points in the high latitude southern hemisphere largely have a salinity peak in austral spring, a forcing peak in late winter, and a forcing combined with advection and entrainment peak in early to mid winter. Grid points in the tropics have a salinity peak in boreal spring and a forcing peak in late winter, which does not change as much as some other areas of the ocean when considering advection and entrainment. This could have to do with the fact that there are fewer significant harmonic fits in the tropics overall. In the high latitude northern hemisphere salinity peaks in early boreal spring, forcing peaks in late winter, and forcing combined with advection and entrainment peaks in early winter.

313

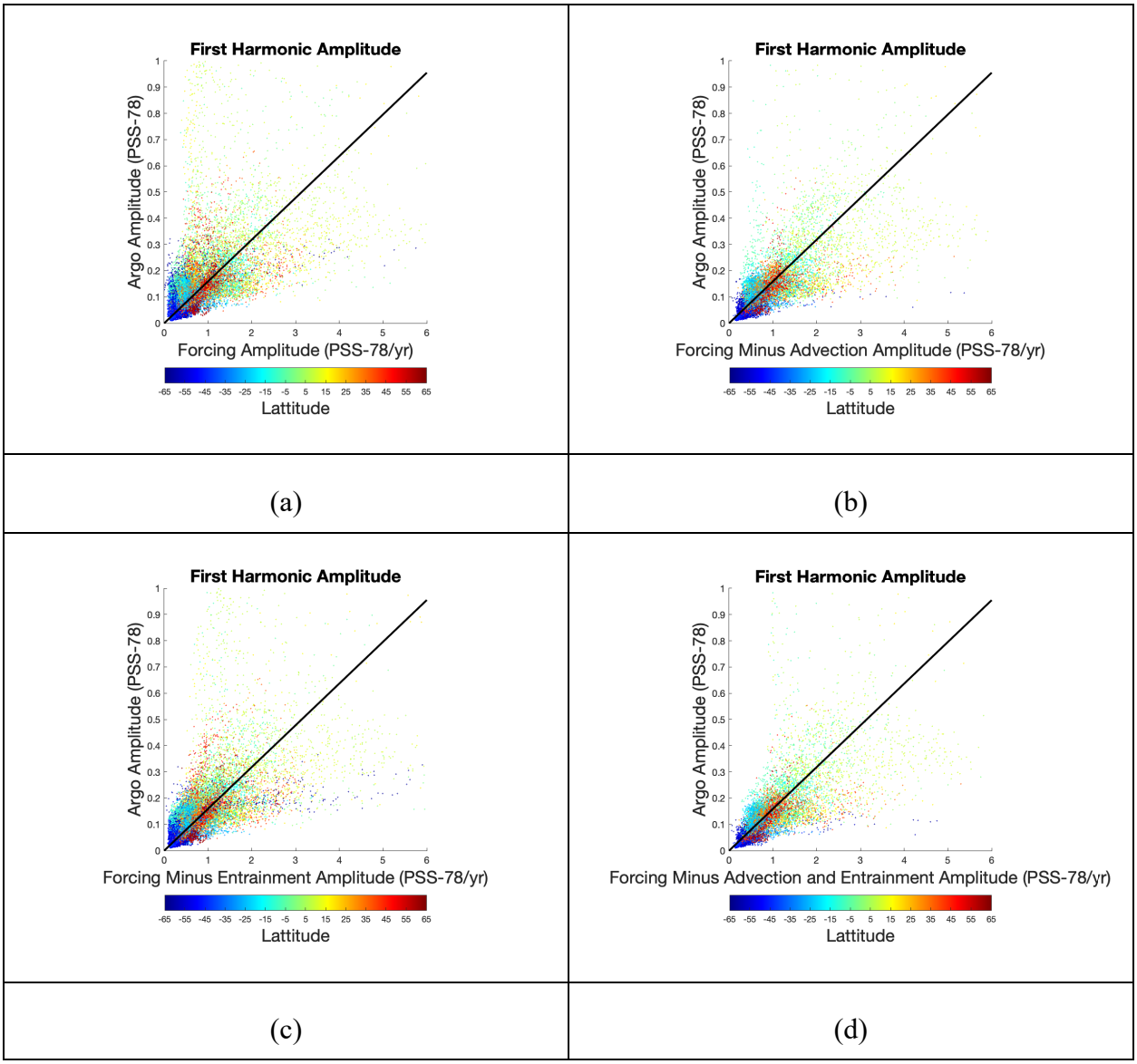

314 **Figure 4:** (a) Scatterplot comparison of seasonal first harmonic amplitude for RG vs. FWF. Each symbol is for one
315 grid point, with symbols plotted only where there is a significant fit for both RG and FWF. Colors of symbols
316 indicate latitude of each point with scale at bottom. A black line shows the correspondence expected if the FWF
317 totally determined the SSS, i.e. with a slope of $1/2\pi$. (b) Same as (a) but for RG vs. FWF combined with advection.
318 (c) Same as (a) but for Argo SIO vs. FWF combined with entrainment. (d) Same as (a) but for RG vs. FWF
319 combined with advection and entrainment.

320 The scatter plots in Figure 4 are formatted in the same manner as Figure 3, but with the annual
321 harmonic amplitude plotted for surface salinity and various combinations of forcing terms. The
322 black line shows the expected slope of $\frac{1}{2\pi}$. The patterns in amplitude are much less clear than the
323 patterns in phase. While none of the scatter plots show the straightforward correspondence
324 predicted by the salinity balance equation, it seems that when not including advection (Figures
325 3a,c) there are more areas of the ocean which have a greater seasonal variation in surface salinity

than would be expected given the freshwater forcing and entrainment. When advection is included there are more areas of the ocean which have a smaller than expected seasonal salinity amplitude given the amplitude of the forcing terms including advection. In addition, adding in advection causes the cloud of points to visually spread less out from the expected line in the scatter plots above. The relationship of amplitude to horizonal advection requires additional research and this paper focuses largely on phase, but it is noteworthy that vertical mixing seems to affect phase more and horizonal advection seems to affect amplitude more. Unlike with the phase, clear patterns with amplitude do not emerge as a function of latitude.

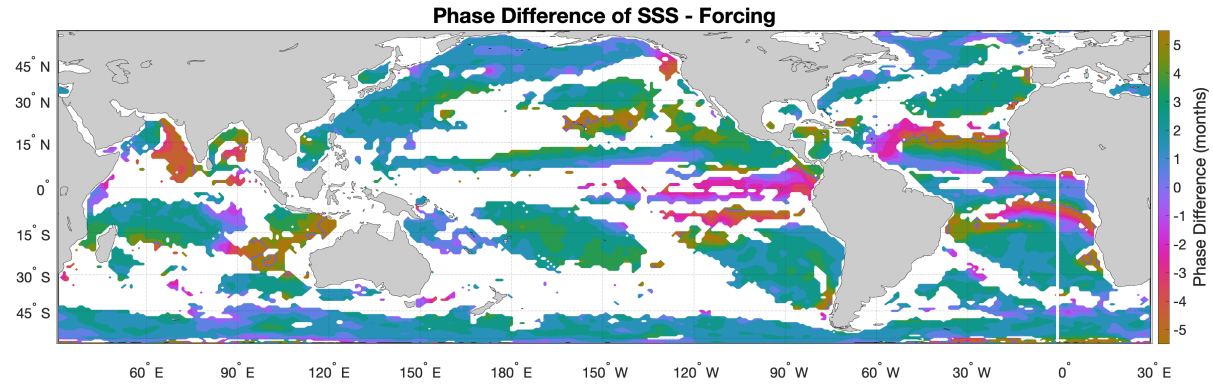
Phase Difference of SSS - Forcing
45° N
30° N
15° N
0°
15° S
30° S
45° S
60° E
90° E
120° E
150° E
180° E
150° W
120° W
90° W
60° W
30° W
0°
30° E
Phase Difference (months)
5
4
3
2
1
0
-1
-2
-3
-4
-5

(a)

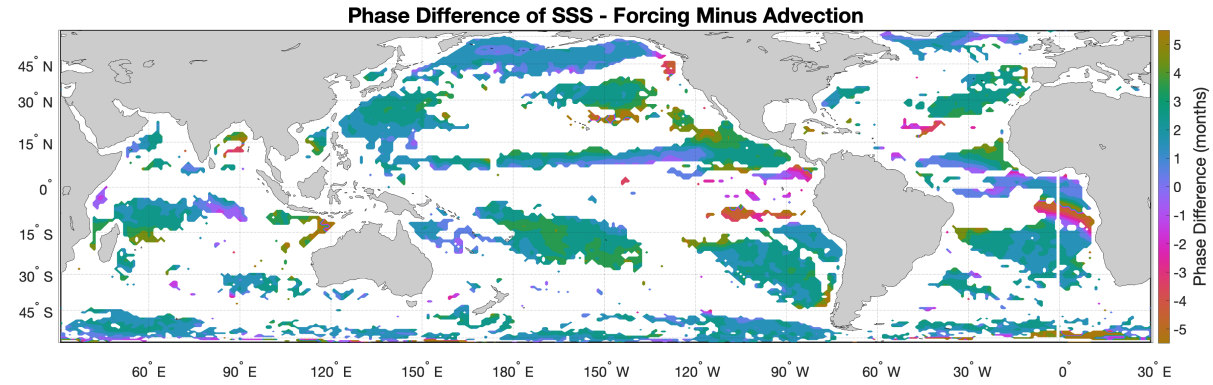
Phase Difference of SSS - Forcing Minus Advection
45° N
30° N
15° N
0°
15° S
30° S
45° S
60° E
90° E
120° E
150° E
180° E
150° W
120° W
90° W
60° W
30° W
0°
30° E
Phase Difference (months)
5
4
3
2
1
0
-1
-2
-3
-4
-5

(b)

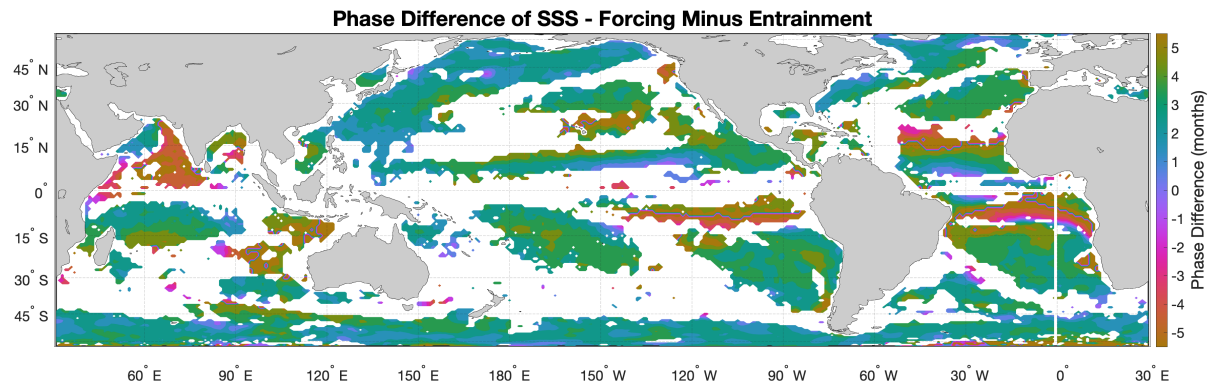
Phase Difference of SSS - Forcing Minus Entrainment
45° N
30° N
15° N
0°
15° S
30° S
45° S
60° E
90° E
120° E
150° E
180° E
150° W
120° W
90° W
60° W
30° W
0°
30° E
Phase Difference (months)
5
4
3
2
1
0
-1
-2
-3
-4
-5

(c)

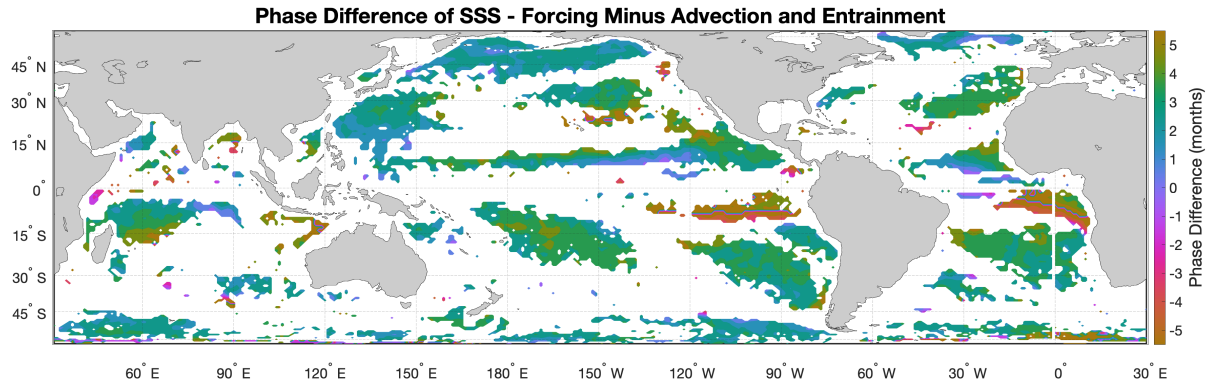

(d)

Figure 5: (a) Map of difference between FWF phase and RG phase (months FWF peaks before SSS peaks). Color indicates months with scale at right. Locations are only plotted where there is a significant fit for both RG and FWF. If the FWF totally determined the SSS, the value of the difference would be 3 months. (b) Same as (a) but for RG phase minus FWF combined with advection phase. (c) Same as (a) but for RG phase minus FWF combined with entrainment phase. (d) Same as (a) but for RG phase minus FWF combined with advection and entrainment phase.

The maps in Figure 5 show in more detail where in the ocean there are statistically significant seasonal harmonics, and where the difference between the phase of sea surface salinity and various forcing terms is close to the expected 3 months. In all of these plots there are relatively few significant fits around the equator and between 20° S and 40° S. The expected 3 month difference is in green. For the comparison between SSS and FWF only, large deviations from that occur in the eastern tropical basins, especially the Pacific, the Arabian Sea, a band around 20°N in the subtropical North Atlantic and a few other scattered locations (Figure 5a). When we include advection (Figure 5b) the number of locations with significant fits decreases sharply, mainly in the eastern tropical Pacific and Southern Ocean. Adding entrainment (Figure 5c) brings many areas closer to the 3 month expected difference, especially in the subtropical South Pacific and western and northern North Pacific. Finally, the inclusion of all terms (Figure 5d) reduces the number of areas with significant fits, but shows that more areas have phase differences close to 3 months.

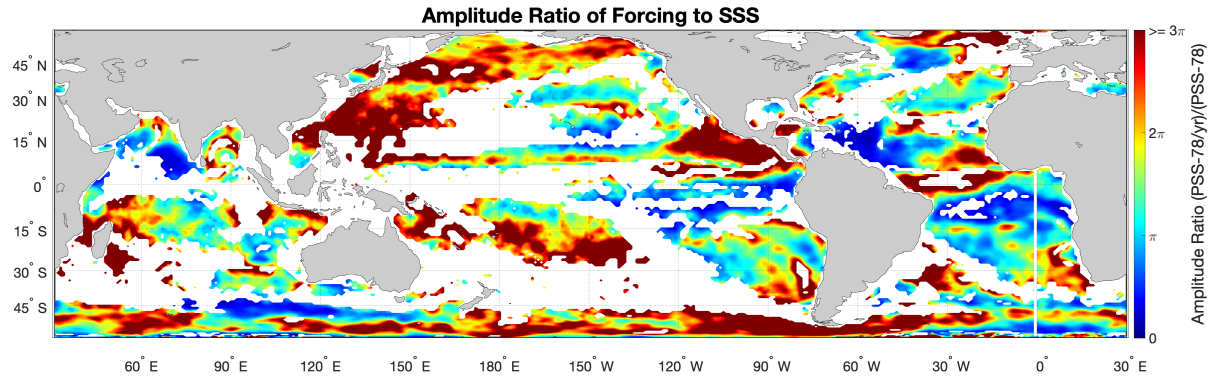
Amplitude Ratio of Forcing to SSS
45° N
30° N
15° N
0°
15° S
30° S
45° S
60° E
90° E
120° E
150° E
180° E
150° W
120° W
90° W
60° W
30° W
0°
30° E
>= 3π
2π
π
0
Amplitude Ratio (PSS-78/yr)/(PSS-78)

(a)

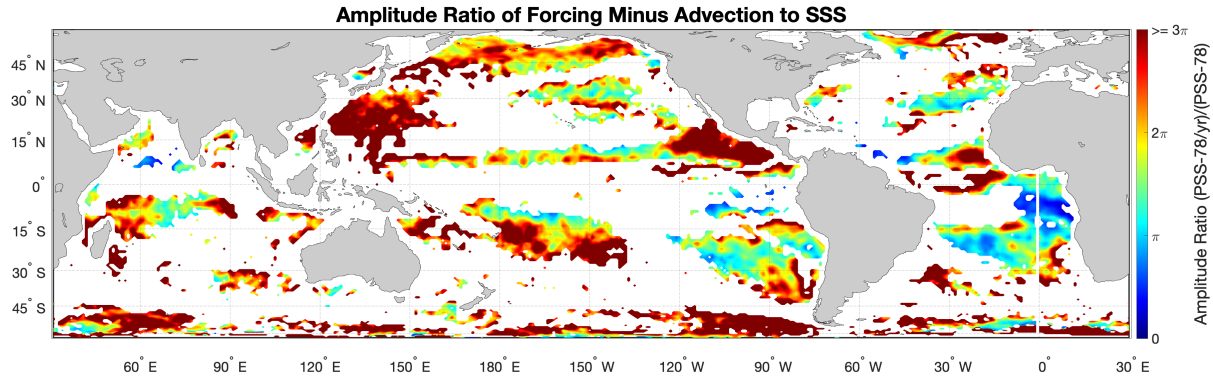
Amplitude Ratio of Forcing Minus Advection to SSS
45° N
30° N
15° N
0°
15° S
30° S
45° S
60° E
90° E
120° E
150° E
180° E
150° W
120° W
90° W
60° W
30° W
0°
30° E
>= 3π
2π
π
0
Amplitude Ratio (PSS-78/yr)/(PSS-78)

(b)

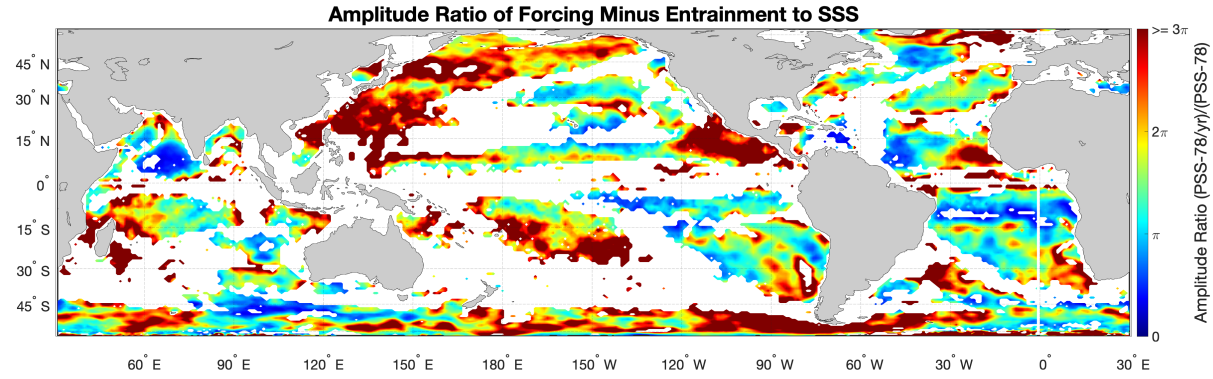
Amplitude Ratio of Forcing Minus Entrainment to SSS
45° N
30° N
15° N
0°
15° S
30° S
45° S
60° E
90° E
120° E
150° E
180° E
150° W
120° W
90° W
60° W
30° W
0°
30° E
>= 3π
2π
π
0
Amplitude Ratio (PSS-78/yr)/(PSS-78)

(c)

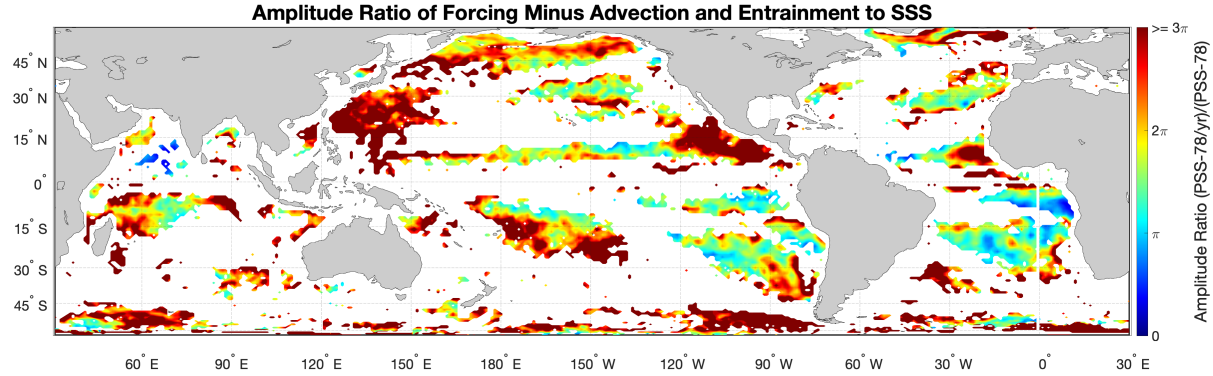

(d)

Figure 6: (a) Map of ratio of FWF amplitude to RG amplitude. Color indicates PSS-78 per year/PSS-78 with scale at right. Locations are only plotted where there is a significant fit for both RG and FWF. If the FWF totally determined the SSS, the value of the ratio would be 2π. (b) Same as (a) but for FWF combined with advection amplitude to RG amplitude. (c) Same as (a) but for FWF combined with entrainment amplitude to RG amplitude. (d) Same as (a) but for FWF combined with advection and entrainment amplitude to RG amplitude.

Figure 6 shows the amplitude ratio of various forcing terms to salinity where there are significant annual harmonic fits. The expected ratio is 2π, i.e. orange in the color scale of the maps. Unilike the maps of phase difference (Figure 5), the amplitude ratios are highly variable. In many areas the amplitude of the forcing terms is large compared to SSS (e.g. the northwestern North Pacific, or the South Pacific Convergence Zone in the western South Pacific). In other areas the SSS has a large amplitude compared to the forcing (e.g. the tropical Atlantic). Adding advection and entrainment does not bring amplitude ratios closer to the expected value (Figures 6b-d).

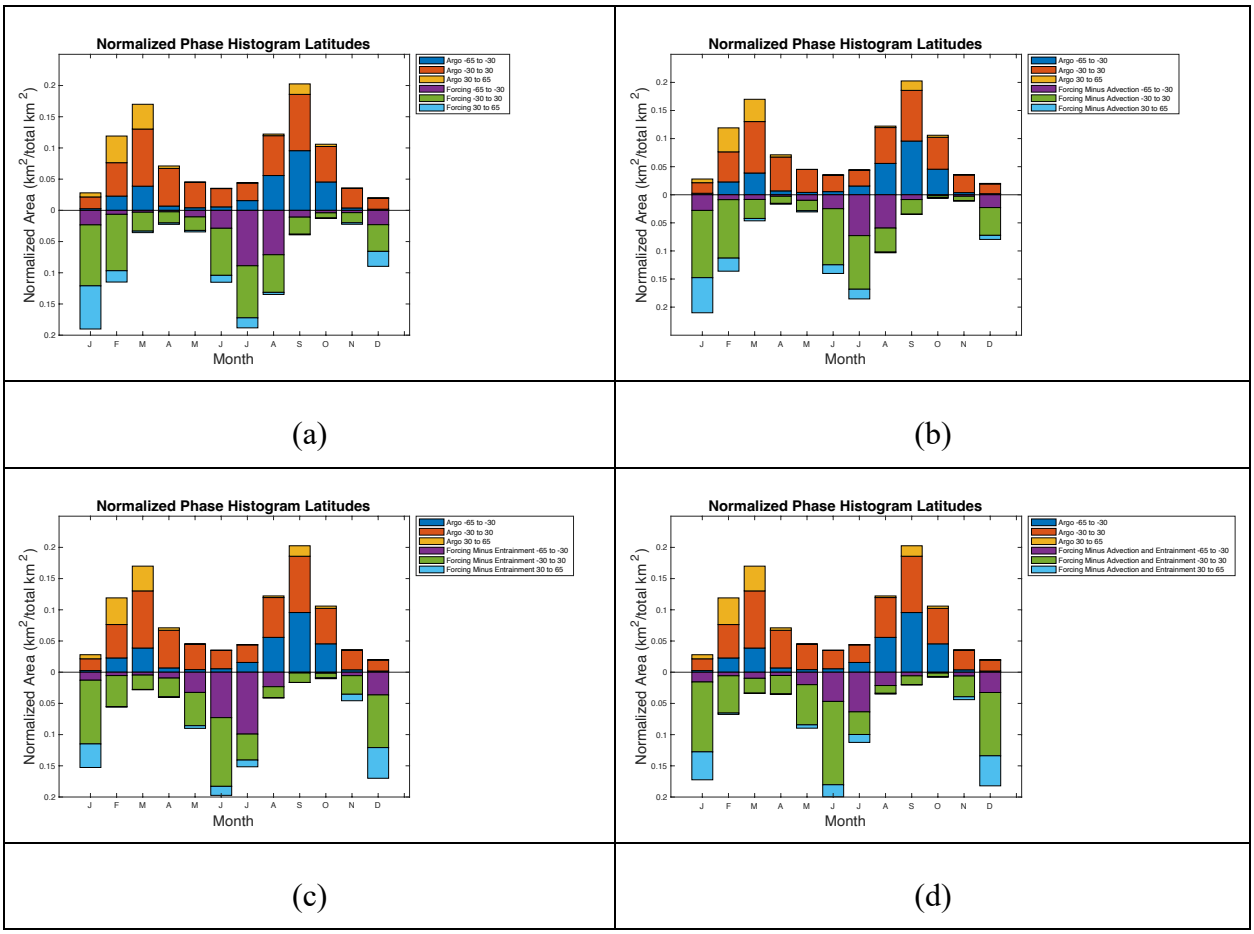

Figure 7: (a) Area where FWF (bottom bars) and SSS (top bars) are maximum for the annual harmonic for different months. Latitude ranges are shown as different colors as indicated in the legends. The units are area normalized by the total area with significant fit. (b) Same as (a) but for FWF combined with advection. (c) Same as (a) but for FWF combined with entrainment. (d) Same as (a) but for FWF combined with advection and entrainment. Note that the upper set of bars is the same for each panel.

The area where SSS and various forcing terms peak is shown in Figure 7. As seen in the scatterplots of Figure 3, SSS peaks in mainly in March and September. This is true for all latitude ranges. For high southern latitudes (dark blue bars) there is a clear peak in September - spring. In the tropics (30°S-30°N, red bars) the peaks are in both March and September, but with less seasonal variation. For higher northern latitudes (yellow bars) the peak is in February and March, i.e. late winter/early spring.

With just FWF and no ocean dynamics (Figure 6a, lower bars) the FWF peaks in January and July. The July peak is associated with high southern latitudes (purple bars). In the tropics (green bars) the peaks are in January and July, and in higher northern latitudes, the peaks are in January. The higher latitude peaks indicate maxima in E-P possibly due to intense evaporation that occurs in western boundary current regions such as the Gulf Stream or Kuroshio in winter (Large & Yeager, 2009; Hsiung, 1986).

As ocean dynamics are added (Figure 7b-d) the peaks in forcing shift to earlier months. The July peak in panel a especially shifts back in time to June when entrainment is included (panels c and d) but not as much for only advection (panel b). The January peak in panel a shifts back to December/January with the inclusion of entrainment and (to a lesser extent) advection. These shifts are visible at all latitude ranges.

4 Discussion

We have computed annual harmonics of various terms of the upper ocean salinity balance equation, focusing mainly on the phase relationship between the terms and the salinity itself. We briefly discuss the relationship of the amplitudes (Figures 4 and 6), but find much less definitive results and leave more in-depth study of that for future work.

For much of the ocean, where there is a significant annual cycle of SSS, it peaks in the spring at higher latitudes and in March and September in the tropics (Figures 3 and 7). As a whole, this timing of the peak of SSS is likely related to the timing of the peak of E-P, which mainly occurs in the winter at higher latitudes and in January or July in lower latitudes (Figure 7a lower bars). In gross, this freshening and saltening of the surface ocean associated with evaporation and precipitation define the major part of the global water cycle (Schanze et al., 2010). This cycle extracts water from the ocean surface and moves it via the atmosphere from one part of the ocean to another, or from ocean to land, only to have it return to the surface ocean via rainfall or river runoff. The opposite phasing of the tropics and high latitudes suggests an intrahemispheric seasonal transfer of water with fresh water moving poleward in summer, and equatorward in winter. Mean global transport of freshwater has been observed and reported on (Wijffels et al., 1992; Sohail et al., 2022), but not so with the seasonal cycle. The magnitude of this seasonal movement of water and its mechanisms are important subjects for future study.

The freshwater forcing has a clear annual cycle over many parts of the ocean, but is in many places out of balance with the SSS tendency (Figure 5a). When we add in advection and entrainment, other terms on the right-hand-side of equation (1), the phase does rectify and get closer to matching with that of the SSS. However, we also find that areas with large seasonal variability become not statistically significant. This is most true with regions that are out of balance. That is, many of the areas that are pink and brown in Figure 5a, disappear in Figures 5b-d, especially due to advection (Figure 5b). Advection therefore has the effect of moving water out of regions that are strongly seasonal in terms of forcing, and smearing the annual cycle out.

The main conclusion of this paper is that ocean dynamics are required to make the seasonal balance of terms in the upper ocean salinity/freshwater budget close in terms of timing. In particular, vertical entrainment plays a major role in rectifying the seasonal cycle of SSS relative to FWF. As the mixed layer base deepens in fall and winter as part of its annual cycle, it mixes water from the interior into the surface. In the tropics, much of the underlying water is saltier than that at the surface due to the presence of subtropical underwater (O'Connor et al., 2005; Shcmitt & Blair, 2015), so this process increases the salinity of the mixed layer. As such, the results presented here highlight the importance of the subtropical cell of McCreary & Lu (1994) in the global water cycle. Unfortunately, there are no observations of the seasonal variability of the subtropical cell, and little understanding of the role that this cell might play in the seasonal motion of freshwater.

Data Availablility Statement:

Data used in this paper can be obtained from the following sources:

- RG Argo Data https://sio-argo.ucsd.edu/RG_Climatology.html
- OAFlux evaporation https://climatedataguide.ucar.edu/climate-data/oaflux-objectively-analyzed-air-sea-fluxes-global-oceans
- MIMOC mixed layer depth https://www.pmel.noaa.gov/mimoc/
- GPM IMERG precipitation https://gpm.nasa.gov/data/imerg
- OSCAR surface velocity https://podaac.jpl.nasa.gov/dataset/OSCAR_L4_OC_third-deg
- NOAA Coastwatch Ekman upwelling https://coastwatch.pfeg.noaa.gov/erddap/griddap/erdQAstressmday.html

Acknowledgments

The authors certify they do not have any real or perceived conflicts of interest. This research was supported by NASA under grants 19-OSST19-0007 and 80NSSC18K1322.

References

Bingham, F. M., S. Brodnitz, and L. Yu (2021), Sea Surface Salinity Seasonal Variability in the Tropics from Satellites, Gridded In Situ Products and Mooring Observations, Remote Sensing, 13(1), 110, doi:10.3390/rs13010110.

Bingham, F. M., J. Busecke, A. L. Gordon, C. F. Giulivi, and Z. Li (2014), The North Atlantic subtropical surface salinity maximum as observed by Aquarius, Journal of Geophysical Research: Oceans, 119(11), 7741-7755, doi:10.1002/2014JC009825.

Bingham, F. M., G. R. Foltz, and M. J. McPhaden (2010), Seasonal cycles of surface layer salinity in the Pacific Ocean, Ocean Science, 6, 775-787, doi:10.5194/os-6-775-2010.

Bingham, F. M., G. R. Foltz, and M. J. McPhaden (2012), Characteristics of the Seasonal Cycle of Surface Layer Salinity in the Global Ocean, Ocean Science, 8, 915-929, doi:10.5194/os-8-915-2012.

Bingham, F. M., and T. Lee (2017), Space and time scales of sea surface salinity and freshwater forcing variability in the global ocean (60° S–60° N), Journal of Geophysical Research: Oceans, 122(4), 2909-2922, doi:10.1002/2016JC012216.

Bonjean, F., and G. S. Lagerloef (2002), Diagnostic Model and Analysis of the Surface Currents in the Tropical Pacific Ocean, Journal of Physical Oceanography, 32(10), 2938-2954.

Boyer, T. P., and S. Levitus (2002), Harmonic Analysis of Climatological Sea Surface Salinity, Journal of Geophysical Research, 107(C12), 8006, doi:8010.1029/2001JC000829.

Camara, I., N. Kolodziejczyk, J. Mignot, A. Lazar, and A. T. Gaye (2015), On the seasonal variations of salinity of the tropical Atlantic mixed layer, Journal of Geophysical Research: Oceans, 120(6), 4441-4462, doi:10.1002/2015JC010865.

Chambers, D. P., J. Wahr, and R. S. Nerem (2004), Preliminary observations of global ocean mass variations with GRACE, Geophysical Research Letters, 31, 13310, doi:1029/12004GL020461.

Chen, G., L. Peng, and C. Ma (2018), Climatology and seasonality of upper ocean salinity: a three-dimensional view from argo floats, Climate Dynamics, 50(5), 2169-2182, doi:10.1007/s00382-017-3742-6.

Da-Allada, C. Y., G. Alory, Y. du Penhoat, E. Kestenare, F. Durand, and N. M. Hounkonnou (2013), Seasonal mixed-layer salinity balance in the tropical Atlantic Ocean: Mean state and seasonal cycle, Journal of Geophysical Research: Oceans, 118(1), 332-345, doi:10.1029/2012JC008357.

Da-Allada, C. Y., Y. du Penhoat, J. Jouanno, G. Alory, and N. M. Hounkonnou (2014), Modeled mixed-layer salinity balance in the Gulf of Guinea: seasonal and interannual variability, Ocean Dynamics, 64(12), 1783-1802, doi:10.1007/s10236-014-0775-9.

Da-Allada, C. Y., F. Gaillard, and N. Kolodziejczyk (2015), Mixed-layer salinity budget in the tropical Indian Ocean: seasonal cycle based only on observations, Ocean Dynamics, 65(6), 845-857, doi:10.1007/s10236-015-0837-7.

Delcroix, T., C. Henin, V. Porte, and P. Arkin (1996), Precipitation and Sea-surface Salinity in the Tropical Pacific, Deep-Sea Research I, 43(7), 1123-1141.

Dessier, A., and J. R. Donguy (1994), The sea surface salinity in the Tropical Atlantic between 10 degree S and 30 degree N -- seasonal and interannual variations (1977-1989), Deep-Sea Research A, 41(11994 Issn 0967-0637 English Journal Article ASFA 2: Ocean Technology Policy & Non-Living Resources; Oceanic Abstracts), 81-100.

Dohan, K., H.-Y. Kao, and G. S. E. Lagerloef (2015), The freshwater balance over the North Atlantic SPURS domain from Aquarius satellite salinity, OSCAR satellite surface currents, and some simplified approaches, Oceanography, 28(1), 86–95, doi:10.5670/oceanog.2015.07.

Dong, S., S. L. Garzoli, and M. Baringer (2009), An assessment of the seasonal mixed layer salinity budget in the Southern Ocean, Journal of Geophysical Research: Oceans, 114(C12), doi:10.1029/2008JC005258.

Dong, S., G. Goni, and R. Lumpkin (2015), Mixed-layer salinity budget in the SPURS region on seasonal to interannual time scales, Oceanography, 28(1), 78–85, doi:10.5670/oceanog.2015.05.

Donguy, J.-R., and G. Meyers (1996), Seasonal variations of sea-surface salinity and temperature in the tropical Indian Ocean, Deep Sea Research Part I: Oceanographic Research Papers, 43(2), 117-138, doi:10.1016/0967-0637(96)00009-X.

Farrar, J. T., and A. J. Plueddemann (2019), On the Factors Driving Upper-Ocean Salinity Variability at the Western Edge of the Eastern Pacific Fresh Pool, Oceanography, 32, doi:10.5670/oceanog.2019.209.

Farrar, J. T., et al. (2015), Salinity and temperature balances at the SPURS central mooring during fall and winter, Oceanography, 28(1), 56–65, doi:10.5670/oceanog.2015.06.

Foltz, G. R., S. Grodsky, D. Cayan, and M. McPhaden (2004), Seasonal salt budget of the northwestern tropical Atlantic Ocean along 38°W, Journal Geophysical Research C Oceans, 109, C03052, doi:10.1029/2003JC002111.

Foltz, G. R., and M. J. McPhaden (2008), Seasonal Mixed Layer Salinity Balance of the Tropical North Atlantic Ocean, Journal of Geophysical Research.C.Oceans, 113, C02013, doi:02010.01029/02007JC004178.

Gordon, A. L., C. F. Giulivi, J. Busecke, and F. M. Bingham (2015), Differences among subtropical surface salinity patterns, Oceanography, 28(1), 32–39, doi:10.5670/oceanog.2015.02.

Hasson, A., T. Delcroix, and J. Boutin (2013a), Formation and variability of the South Pacific Sea Surface Salinity maximum in recent decades, Journal of Geophysical Research Oceans, 118(10), 5109-5116, doi:10.1002/jgrc.20367.

Hasson, A., T. Delcroix, J. Boutin, R. Dussin, and J. Ballabrera-Poy (2013b), Analysing the 2010-2011 La Niña signature in the tropical Pacific sea surface salinity using in situ, SMOS observations and a numerical simulation, Journal of Geophysical Research - Oceans, 119, 3855–3867, doi:10.1002/2013JC009388.

Hoffman, L., M. R. Mazloff, S. T. Gille, D. Giglio, and A. Varadarajan (2022), Ocean Surface Salinity Response to Atmospheric River Precipitation in the California Current System, Journal of Physical Oceanography, 52(8), 1867-1885, doi:10.1175/jpo-d-21-0272.1.

Hsiung, J. (1986), Mean surface energy fluxes over the global ocean, Journal of Geophysical Research: Oceans, 91(C9), 10585-10606, doi:10.1029/JC091iC09p10585.

Huang, R. X., and R. W. Schmitt (1993), The Goldsbrough–Stommel Circulation of the World Oceans, Journal of Physical Oceanography, 23(6), 1277-1284, doi:10.1175/1520-0485(1993)023<1277:tgcotw>2.0.co;2.

Johnson, B. K., F. O. Bryan, S. A. Grodsky, and J. A. Carton (2016), Climatological Annual Cycle of the Salinity Budgets of the Subtropical Maxima, Journal of Physical Oceanography, 46(10), 2981-2994, doi:10.1175/JPO-D-15-0202.1.

Kraus, E. B., and J. S. Turner (1967), A one-dimensional model of the seasonal thermocline II. The general theory and its consequences, Tellus, 19(1), 98-106, doi:10.3402/tellusa.v19i1.9753.

Köhler, J., N. Serra, F. O. Bryan, B. K. Johnson, and D. Stammer (2018), Mechanisms of Mixed-Layer Salinity Seasonal Variability in the Indian Ocean, Journal of Geophysical Research: Oceans, 123(1), 466-496, doi:10.1002/2017JC013640.

Large, W. G., and S. G. Yeager (2009), The global climatology of an interannually varying air–sea flux data set, Climate Dynamics, 33(2), 341-364, doi:10.1007/s00382-008-0441-3.

Levitus, S. (1986), Annual Cycle of Salinity and Salt Storage in the World Ocean, Journal of Physical Oceanography, 16(2), 322-343, doi:10.1175/1520-0485(1986)016<0322:acosas>2.0.co;2.

546 Maes, C., and T. J. O'Kane (2014), Seasonal variations of the upper ocean salinity stratification
547 in the Tropics, Journal of Geophysical Research: Oceans, 119(3), 1706-1722,
548 doi:10.1002/2013JC009366.

549 McCreary, J., and P. Lu (1994), On the Interaction between the Subtropical and Equatorial
550 Ocean Circulations: The Subtropical Cell, Journal of Physical Oceanography, 24, 466-
551 497.

552 Minster, J. F., A. Ceznave, Y. V. Serafini, F. Mercier, M. C. Gennero, and P. Rogel (1999),
553 Annual cycle in mean sea level from Topex–Poseidon and ERS-1: inference on the global
554 hydrological cycle, Global and Planetary Change, 20(1), 57, doi:10.1016/S0921-
555 8181(1098)00058-00057.

556 Rao, R. R., and R. Sivakumar (2003), Seasonal variability of sea surface salinity and salt budget
557 of the mixed layer of the north Indian Ocean, Jour. Geophys. Res. C Oceans, 108(C1),
558 3009, doi:3010.1029/2001JC000907.

559 Reverdin, G., E. Kestenare, C. Frankignoul, and T. Delcroix (2007), Surface salinity in the
560 Atlantic Ocean (30°S–50°N), Prog. Oceanogr., 73, 311-340,
561 doi:10.1016/j.pocean.2006.11.004.

562 Roemmich, D., and J. Gilson (2009), The 2004–2008 mean and annual cycle of temperature,
563 salinity, and steric height in the global ocean from the Argo Program, Progress in
564 Oceanography, 82, 81, doi:10.1016/j.pocean.2009.1003.1004.

565 Schanze, J. J., R. W. Schmitt, and L. L. Yu (2010), The global oceanic freshwater cycle: A state-
566 of-the-art quantification, Journal of Marine Research, 68(3-1), 569-595,
567 doi:10.1357/002224010794657164.

568 Schmidtko, S., G. C. Johnson, and J. M. Lyman (2013), MIMOC: A global monthly isopycnal
569 upper-ocean climatology with mixed layers, Journal of Geophysical Research Oceans,
570 118(4), 1658-1672, doi:10.1002/jgrc.20122.

571 Sena Martins, M., N. Serra, and D. Stammer (2015), Spatial and temporal scales of sea surface
572 salinity variability in the Atlantic Ocean, Journal of Geophysical Research Oceans, 120,
573 4306–4323, doi:10.1002/2014JC010649.

574 Skofronick-Jackson, G., et al. (2017), The Global Precipitation Measurement (GPM) Mission for
575 Science and Society, Bulletin of the American Meteorological Society, 98(8), 1679-1695,
576 doi:10.1175/BAMS-D-15-00306.1.

577 Sohail, T., J. D. Zika, D. B. Irving, and J. A. Church (2022), Observed poleward freshwater
578 transport since 1970, Nature, 602(7898), 617-622, doi:10.1038/s41586-021-04370-w.

579 Song, Y. T., T. Lee, J.-H. Moon, T. Qu, and S. Yueh (2015), Modeling skin-layer salinity with
580 an extended surface-salinity layer, Journal of Geophysical Research Oceans, 120(2),
581 1079-1095, doi:10.1002/2014JC010346.

582 Vinogradova, N., et al. (2019), Satellite Salinity Observing System: Recent Discoveries and the
583 Way Forward, Frontiers in Marine Science, 6, 243, doi:10.3389/fmars.2019.00243.

584 Vinogradova, N. T., and R. M. Ponte (2013), Clarifying the link between surface salinity and
585 freshwater fluxes on monthly to interannual time scales, Journal of Geophysical Research
586 Oceans, 118(6), 3190-3201, doi:10.1002/jgrc.20200.

Wang, Y., Y. Li, and C. Wei (2020), Subtropical sea surface salinity maxima in the South Indian Ocean, Journal of Oceanology and Limnology, 38(1), 16-29, doi:10.1007/s00343-019-8251-5.

Wijffels, S., R. Schmitt, H. Bryden, and A. Stigebrandt (1992), Transport of Freshwater by the Oceans, Journal of Physical Oceanography, 22, 155-162.

Yu, L. (2011), A global relationship between the ocean water cycle and near-surface salinity, Journal of Geophysical Research: Oceans, 116(C10), C10025, doi:10.1029/2010JC006937.

Yu, L., F. M. Bingham, T. Lee, E. P. Dinnat, S. Fournier, O. Melnichenko, W. Tang, and S. H. Yueh (2021), Revisiting the Global Patterns of Seasonal Cycle in Sea Surface Salinity, Journal of Geophysical Research: Oceans, 126(4), e2020JC016789, doi:10.1029/2020JC016789.

Yu, L., and R. A. Weller (2007), Objectively Analyzed Air–Sea Heat Fluxes for the Global Ice-Free Oceans (1981–2005), Bulletin of the American Meteorological Society, 88(4), 527-539, doi:10.1175/BAMS-88-4-527.